http://dx.doi.org/10.5012/bkcs.2011.32.11.3904

Synthesis, Structure, and Peroxidase Activity of an Octahedral Ru(III) Complex with a Tripodal Tetraamine Ligand

Jang-Hoon Cho, Kwan Mook Kim,† Dong-Youn Noh,‡ and Hong-In Lee*

*Department of Chemistry and Green-Nano Materials Research Center, Kyungpook National University, Daegu 702-701, Korea. *E-mail: leehi@knu.ac.kr*
†Department of Chemistry and Nano Sciences, Ewha Womans University, Seoul 120-750, Korea
‡Department of Chemistry, Seoul Women's University, Seoul 139-774, Korea
Received July 25, 2011, Accepted September 6, 2011

A new octahedral Ru(III) complex with a tripodal tetraamine ligand, tpea = tris[2-(1-pyrazoyl)ethyl]amine, has been prepared and characterized. The single crystal X-ray crystallographic study of the complex revealed that the complex has a near octahedral geometry with the tetradentate ligand and two chloride ions. Peroxidase activity was examined by observing the oxidation of 2,2'-azinobis(3-ethylbenzothiazoline)-6-sulfonic acid (ABTS) with hydrogen peroxide in the presence of the complex. Amount of $ABTS^{+\bullet}$ generated during the reaction was monitored by UV/VIS and EPR spectroscopies. After the initiation of the peroxidase reaction, $ABTS^{+\bullet}$ concentration increases and then decreases after certain time, indicating that both ABTS and $ABTS^{+\bullet}$ are the substrates of the peroxidase activity of the Ru(III) complex.

Key Words : Ruthenium(III) complex, Antioxidant, Tetradentate ligand, Crystal structure

Introduction

Ruthenium complexes have been widely developed to be applied for pharmaceuticals,[1] precursors in a variety of inorganic syntheses,[2] oxo-transfer catalysts,[3] photoinduced energy,[4] water oxidation,[5] and others. Especially, recent advances in the pharmaceutical applications of Ru(III) complexes as anticancer drugs have brought much attention to new developments of Ru(III) compounds.[6-10] Among those, octahedral Ru(III) complexes with chloride and heterocyclic azole ligands have shown promising results.[7-10]

For the clinical success of the complexes, understanding the reactivities of the biomolecule-bound Ru(III) complexes is necessitated. Because these anticancer octahedral Ru(III) complexes tend to selectively bind to imine sites, such as the histidyl imidazole nitrogens on proteins and the N7 sites on the imidazole ring of the purine nucleotides, by replacing the chloride ligands,[1] we have looked for the ligands which can provide at least three heterocyclic azole groups and also form an octahedral complexes. Tris(2-(1-pyrazolyl)ethyl)-amine (tpea) containing three pyrazole groups is a potentially tetradentate tripodal tetraamine ligand. Several metal complexes with the tpea ligand have been synthesized and they usually have formed four or five coordinated complexes.[11] However, two factors attracted us to choose the ligand as a candidate for the octahedral Ru(III) model complex: strong tendencies (i) toward the six-coordination of Ru ions and (ii) the formation of six-membered chelate rings with near perpendicular bite angles of tpea upon coordination. In this study, we have used the tpea ligand to synthesize a new model octahedral Ru(III) complex and investigated its structure and physiological reactivity.

Experimental

Materials. Following chemicals were purchased from commercial sources and were used without further purification: Pyrazole, tris(2-chloroethyl)amine hydrochloride, potassium[aquapentachloro-rutheniumate(III)], and the diammonium salt of 2,2'-azinobis(3-ethylbenzothiazoline)-6-sulfonic acid (ABTS) from Sigma-Aldrich Chemical, and hydrogen peroxide from Junsei Chemical. All solvents were purified before use according to the standard procedures.

Physical Measurements. NMR (400 MHz) spectra were recorded on a Bruker Advance Digital 400-NMR spectrometer and chemical shifts were recorded in ppm units. Fourier transform infrared (FT-IR) spectra of samples were recorded with a Bruker IFS 66v FT-IR spectrophotometer in the region of 400 cm^{-1} to 4000 cm^{-1} using KBr pellets and visible electronic spectra were recorded with a Scinco UV S-2100 spectrophotometer. The elemental analysis was done using a Perkin-Elmer 2400 CHN analyzer. X-Band (9 GHz) EPR spectra were recorded on a Jeol JES-TE300 ESR spectrometer using 100 kHz field modulation. Low temperature EPR spectra were obtained using a Jeol ES-DVT3 variable temperature controller. Cyclic voltammetry (CV) was carried out at room temperature with a CHI 620A Electrochemical Analyzer (CHI Instrument Inc.) on 1 mM samples in 3.0 mL CH_3CN, with 0.1 M n-$Bu_4N{\cdot}ClO_4$ as supporting electrolyte. Redox potentials were measured relative to an Ag/Ag^+ reference electrode and determined as potential *vs* ferrocene/ferrocenium (Fc/Fc^+) redox couple.

Preparation of tris[2-(1-pyrazoyl)ethyl]amine (tpea). The tripodal ligand, tris[2-(1-pyrazoyl)ethyl]amine, was prepared under a nitrogen atmosphere according to the literature

method with a slight modification as follows.[12] 2.87 g (73 mmol) of sliced potassium was added slowly to a solution of 5.0 g (73 mmol) of dry pyrazole in 150 mL of dry THF. After the solution was stirred for 6 hrs at RT and then 3 hrs at 60 °C, 50 mL of dry THF was additionally added into the solution. 5.06 g (21 mmol) of tris(2-chloroethyl)amine hydrochloride was slowly added to the resulting suspension. The mixture was stirred vigorously for 60 hrs at 60 °C. The residue obtained from vacuum evaporation of the solution was treated with 100 mL of water, and the solution was extracted with three 75 mL portions of benzene. The yellow combined organic portion (benzene portion) was washed twice with 50 mL each of a saturated aqueous NaCl solution and then dried over Na_2SO_4. The solvent was evaporated to yellow oil. ^{1}H NMR in ppm ($CDCl_3$): 2.86-2.88 (t, 6H, CH_2), 3.82-3.83 (t, 6H, CH_2), 6.11 (t, 3H, pyrazole), 6.74 (d, 3H, pyrazole), 7.35 (d, 3H, pyrazole); ^{13}C NMR in ppm ($CDCl_3$): 51 (CH_2), 55 (CH_2), 105 (pyrazole), 128-131 (pyrazole), 140 (pyrazole).

Synthesis of [Ru(III)(tpea)Cl$_2$]ClO$_4$ (1). A solution of 0.50 g (1.7 mmol) of the ligand tpea in 100 mL ethanol was added dropwise to an 100 mL ethanolic suspension of $K_2[RuCl_5(H_2O)]$ (0.5 g, 1.3 mmol) for 3 hrs at RT. The mixture was further refluxed for 1 day at 100 °C. This was filtered and the filtrate was evaporated to be concentrated. After a few droplets of a saturated aqueous solution of $NaClO_4$ was added to the concentrated solution, the perchlorate salt of $[Ru(III)(tpea)Cl_2]^+$ precipitated as a yellow solid. (Scheme 1) Crystals suitable for X-ray analysis were obtained at the interface of diethyl ether and the methylene chloride solution of the precipitates after 2-3 days. Elemental analysis calculated for $C_{15}H_{21}Cl_3N_7O_4Ru$ (mol. wt. = 570.81): C, 31.56%; H, 3.71%; N, 17.18%. Found: C, 31.38%; H, 3.84%; and N 16.80%. FAB MS analysis: *m/z*, ion, base; (+ ion mode) 471.05, $[Ru(III)(tpea)Cl_2]^+$, 100%. IR (KBr, cm^{-1}): 3437 (NH), 3125 (CH), 1631, 1273 (δHNH), 1413 (CH_2), 1093, 626 (ClO).

X-ray Crystallographic Data Collection and Refinement of the Structure. A yellow crystal of complex **1** was sealed in a thin walled glass capillary and the diffraction data were measured at 293 K on an Enraf-Nonius CAD-4 diffractometer using MoKα (λ = 0.71073 Å). The crystal structure of complex **1** was solved by the direct method and refined by full-matrix least-squares calculation with the SHELXTL software package.[13] A summary of the crystal and some crystallographic data are given in Table S1. Supplementary crystallographic data (CIF), CCDC-833079, for complex **1** can be obtained free of charge at www.ccdc.cam.ac.uk/conts/retrieving.html or from the Cambridge Crystallographic Data Centre, 12, Union Road, Cambridge CB2 1EZ, UK (fax:+44 1223 336033, e-mail: deposit@ccdc.cam.ac.uk).

Peroxidase-activity Test. Peroxidase activity of the complex was tested by observing the oxidation of the ABTS with H_2O_2 in the presence of the complex.[14-17] The reaction was initiated by adding 50 μL of the aqueous solution of H_2O_2 (4.0×10^{-4} mol) into 3 mL of an aqueous solution containing complex **1** (1.0×10^{-8} mol) and ABTS (4.5×10^{-7} mol). The formation of the $ABTS^{+\bullet}$ cation is followed by the absorption peak at λ_{max} = 650 nm (ε = 12000 M^{-1}cm^{-1}).

Results and Discussion

Crystal structure of [Ru(III)(tpea)Cl$_2$]ClO$_4$. Complex **1** crystallizes as a racemic compound in space group $P2_1/b2_1/c2_1/a$ (*Pbca*). Table S1 summarizes the crystal and refinement data. The unit cell contains four enantiomer pairs and eight perchlorate ions. Overall the structure of the crystal can be viewed as a composition of $[Ru(III)(tpea)Cl_2]ClO_4$. The oxidation number of ruthium ion is also confirmed by EPR spectrum of complex **1** (see Figure 5). Figure 1 shows the ORTEP drawing of one of the $[Ru(III)(tpea)Cl_2]^+$ cation enantiomer pair. The tpea ligand tetradentately coordinates to Ru(III) ion through three pyrazol N atoms and one tertiary N atom. Two chloride ions occupy the remaining sites of the octahedral geometry. This kind of Ru(III) complexes with tetradentate tripodal tetraamine ligands has been structurally characterized.[18-22] For complex **1**, the chelation of the ligand forming six-membered rings gives rise to the near octahedral geometry with the bond angles around the Ru(III) ion close to the perpendicular angles as in Table 1 (87.1(2)-95.1(3)° and 176.2(3)-177.2(3)°). The bond length between the Ru(III) ion and the apical tertiary amine N atom of the ligand (2.165(9) Å) is longer than those between the Ru(III) ion and the pyrazol N atoms (2.037(9)-2.068(8) Å). This would be explained by the σ-basicity of the donor N atoms

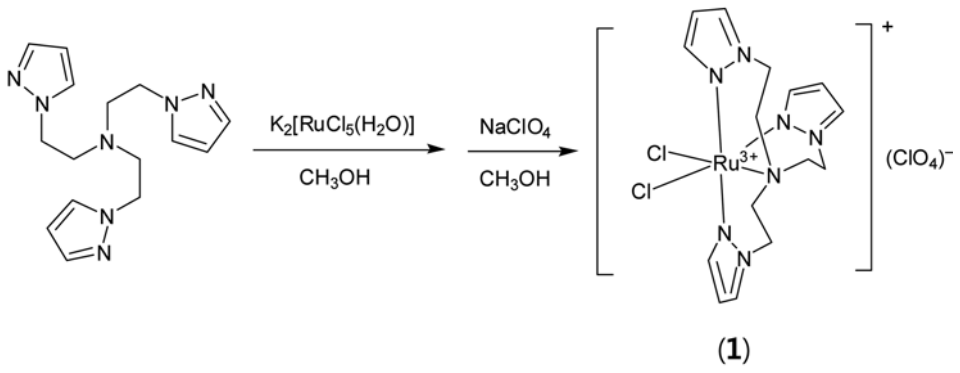

(**1**)

Scheme 1

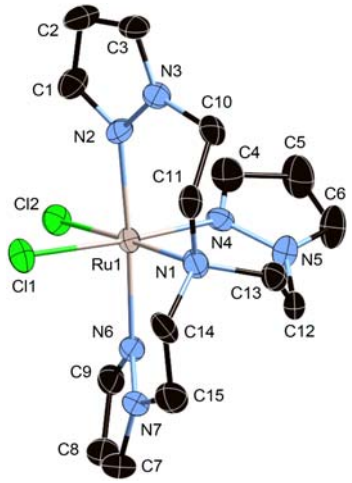

Figure 1. ORTEP diagram of $[Ru(III)(tpea)Cl_2]^+$ of complex **1** with 30% probability ellipsoids and atom numbering scheme. Hydrogen atoms have been omitted for clarity.

Table 1. Selected bond lengths [Å] and angles [°] for $[Ru(III)(tpea)Cl_2]ClO_4$ (**1**)

Bond lengths (Å)			
Ru1-N1	2.165(9)	Ru1-N2	2.068(8)
Ru1-N4	2.037(9)	Ru1-N6	2.068(8)
Ru1-Cl1	2.349(3)	Ru1-Cl2	2.386(3)
Bond angles (°)			
N1-Ru1-N2	95.1(3)	N1-Ru1-N4	89.1(3)
N1-Ru1-N6	87.8(3)	N2-Ru1-N4	89.3(3)
N2-Ru1-N6	176.5(3)	N4-Ru1-N6	92.6(3)
N1-Ru1-Cl1	92.5(3)	N2-Ru1-Cl1	87.1(2)
N4-Ru1-Cl1	176.2(3)	N6-Ru1-Cl1	90.9(2)
N1-Ru1-Cl2	177.2(3)	N2-Ru1-Cl2	87.6(3)
N4-Ru1-Cl2	90.4(3)	N6-Ru1-Cl2	89.4(3)
Cl1-Ru1-Cl2	88.26(10)		

since the Ru(III) ion is not capable of back-bonding. The Ru(III)-$N_{pyrazol}$ bond lengths are comparable to the Ru(III)-$N_{pyridine}$ bond lengths of the reported Ru(III)(tpa) (tpa = tris-(2-pyridylmethyl)amine) complexes: 2.078(5) Å in $[Ru(III)Cl_2(tpa)]ClO_4$ and 2.098(6) Å in $[Ru(III)Cl_2(Metpa)]BF_4$.[21,22] The Ru(III)-Cl bond lengths are the longest in the Ru coordination sphere (2.349(3)-2.386(3) Å). These are close to those found in $[Ru(III)Cl_2(tpa)]ClO_4$ and $[Ru(III)Cl_2(Metpa)]BF_4$ (2.357(2)-2.386(3) Å).[21,22]

The arrangement of the three chelate rings provided by the tripodal ligand tpea cannot generate a chiral conformation.[23] However, the chirality of the complex can arise from the six-membered ligand ring itself.[24] Figure 2 depicts such enantiomer pair present in the crystal of complex **1**. For the conformational analysis of $[Ru(III)(tpea)Cl_2]^+$, it is appropriate to consider the chelate rings as five-membered rings because the connecting $N_{tertiary}$-Ru-$N_{pyrazole}$-$N_{pyrazole}$ atoms in a chelate six-membered ring is near in a plane with some deviations. In that sense, the left of Figure 2 can be viewed as the δλλ ring conformation (N1-C14-C15-N7-N6-Ru1 is the δ conformation) and the right as the λδδ ring conformation.[24]

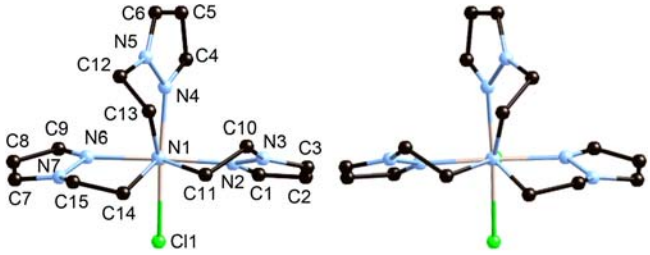

Figure 2. The enantiomer pair of $[Ru(III)(tpea)Cl_2]^+$ with atom numbering scheme. Hydrogen atoms have been omitted for clarity. The figures are the looking-down view through N1-Ru1-Cl2.

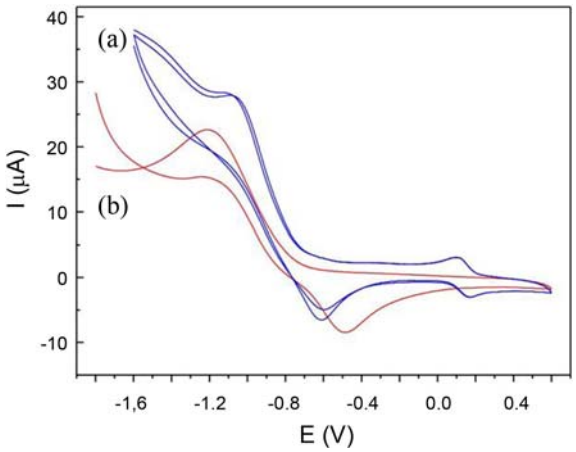

Figure 3. Cyclic voltammograms of (a) 1 mM complex **1** and (b) 1 mM $K_2[Ru(III)(H_2O)Cl_5]$ in 0.1 M (n-Bu_4N)·ClO_4/CH_3CN solution. Scanning rate: 50 mV/s.

Electrochemical Study of $[Ru(III)(tpea)Cl_2]ClO_4$: Figure 3 shows the cyclic voltammograms (CV) of complex **1** and $K_2[Ru(III)(H_2O)Cl_5]$ obtained in CH_3CN with 0.1 M [(n-$Bu)_4N]ClO_4$ electrolyte at room temperature. For $K_2[Ru(III)(H_2O)Cl_5]$, one irreversible process with E_{pa} = –0.49 V and E_{pc} = –1.20 V ascribed to Ru(III)/Ru(II) is observed. In complex **1**, this irreversible Ru(III)/Ru(II) process is observed at E_{pa} = –0.62 V and E_{pc} = –1.07 V. Complex **1** additionally shows a reversible process with $E_{1/2}$ = 135 mV ascribed to Ru(IV)/Ru(III) couple. This redox couple was not observed in $K_2[Ru(III)(H_2O)Cl_5]$ in the range of –2 V to 2 V. This observation indicates that the σ-donating ability of the tpea ligand containing three pyrazoyl groups and one tertiary amine significantly lowers the oxidation potential of Ru(III) ion to be readily oxidized.

Peroxidase Activity: Peroxidase activity of complex **1** was examined by observing the oxidation of ABTS by H_2O_2 in the presence of complex **1** at neutral pH.[14-17] ABTS has been used for the peroxidase-activity test because its oxidized form, $ABTS^{+\bullet}$, is a stable green radical with distinct absorption bands at 420, 650, 740, and 835 nm while the reduced form, ABTS, is colorless.[14-17,25] Figures 4(a) and 4(b) display the UV/VIS absorption spectra of ABTS + H_2O_2 and ABTS + complex **1**, respectively. These featureless spectra were invariant for several hours. Peroxidase-like reaction was initiated by adding 50 μL of an aqueous solu-

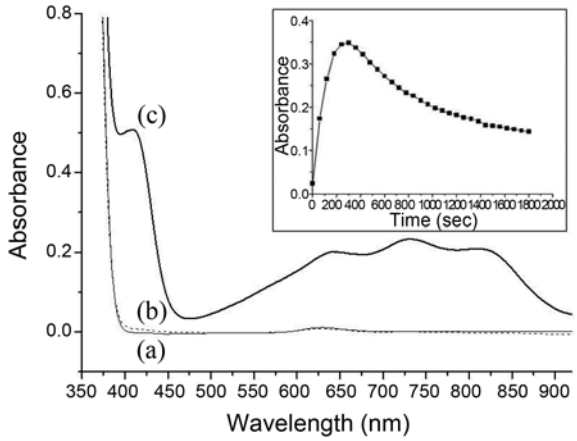

Figure 4. The UV-VIS absorption spectra of (a, thin solid line) ABTS + H_2O_2, (b, dashed line) ABTS + complex **1**, and (c, thick solid line) ABTS + H_2O_2 + complex **1**. In each spectrum, the amounts of ABTS, H_2O_2, and complex **1** are 4.5×10^{-7} mol, 4.0×10^{-4} mol, and 1×10^{-8} mol, respectively, in 3 mL aqueous solution. The spectrum (c) was taken about 100 sec after the reaction initiated by adding 50 μL of an aqueous solution of H_2O_2 (4.0×10^{-4} mol) into 3 mL of an aqueous solution containing complex **1** (1.0×10^{-8} mol) and ABTS (4.5×10^{-7} mol). Inset: the change of the absorbance at λ = 650 nm obtained from the reaction mixture, ABTS + H_2O_2 + complex **1**, from 0 sec to 1800 sec.

tion of H_2O_2 (4.0×10^{-4} mol) into 3 mL of an aqueous solution containing complex **1** (1.0×10^{-8} mol) and ABTS (4.5×10^{-7} mol). The UV/VIS absorption spectrum of ABTS + H_2O_2 + complex **1** taken at about 100 sec after the reaction is shown in Figure 4(c). The spectrum clearly reveals the characteristic bands of $ABTS^{+\bullet}$, indicating that ABTS is oxidized only by complex **1** + H_2O_2. The absorption intensity of $ABTS^{+\bullet}$ starts increasing immediately after the mixing and maximizes at ~300 sec. After that, the intensity gradually decreases. (Inset of Figure 4). The quantitative amount of the oxidized form, $ABTS^{+\bullet}$, can be estimated from the intensity at λ = 650 nm (ε_{650} = 12,000 $cm^{-1}M^{-1}$).[15] The difference between the initial and the maximum intensities at λ = 650 nm indicates that the maximum concentration of $ABTS^{+\bullet}$ is 2.7×10^{-5} M, implying that 8.1×10^{-8} mol of $ABTS^{+\bullet}$ is present at ~300 s after the reaction. Because the initial amount of complex **1** is much less than the maximum amount of $ABTS^{+\bullet}$ and H_2O_2 is excessively present, this clearly shows that complex **1** has a peroxidase activity on ABTS. The decrease of $ABTS^{+\bullet}$ after 300 sec can be explained by further oxidation of $ABTS^{+\bullet}$ to diamagnetic $ABTS^{2+}$, which has no absorption in visible region,[26] by the peroxidase activity of complex **1** on $ABTS^{+\bullet}$.

The generation of $ABTS^{+\bullet}$ was also monitored by electron paramagnetic resonance (EPR). Figure 5 displays the EPR spectra of ABTS and the reaction mixture. The frozen methanolic aqueous solution of complex **1** + ABTS shows a typical rhombic EPR signal with g_1 = 2.263, g_2 = 2.204, and g_3 = 1.852, revealing the low-spin d^5 configuration of the Ru(III) complex.[27] (Figure 5(a)) A narrow and weak signal at g = 2.008 (3252 G) originates from $ABTS^{+\bullet}$ present as an impurity. The spectrum taken at 4 minutes after the reaction

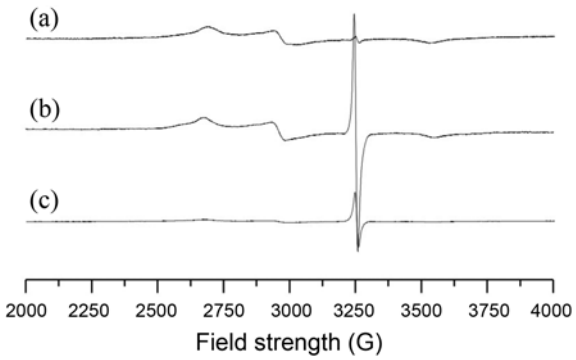

Figure 5. The EPR spectra of (a) complex **1** + ABTS, (b) ABTS + H_2O_2 + complex **1** taken at 4 minutes after the reaction, and (c) ABTS + H_2O_2 + complex **1** taken at 30 minutes after the reaction. The reaction was initiated by adding 50 μL of an aqueous solution of H_2O_2 (4.0×10^{-4} mol) into 3 mL of an methanolic aqueous solution containing complex **1** (1.0×10^{-8} mol) and ABTS (4.5×10^{-7} mol). EPR experimental conditions: microwave frequency, 9.139-9.141 GHz; modulation amplitude, 10 G; modulation frequency, 100 kHz; time constant, 0.3 sec; scan time, 4 minutes; and temperature, 110 K.

initiated by adding H_2O_2 shows the Ru(III) complex signal and a strong EPR signal of $ABTS^{+\bullet}$ generated by the reaction (Figure 5(b)). In the spectrum taken at 30 minutes after the reaction, the rhombic Ru(III) signal is much diminished and the decreased $ABTS^{+\bullet}$ signal is also observed. This observation is consistent with the UV/VIS absorption experiments where the ABTS absorption bands gradually decrease after 300 sec due to further oxidation of $ABTS^{+\bullet}$ to diamagnetic $ABTS^{2+}$.

The UV/VIS absorption and EPR experiments clearly manifest the oxidation of ABTS by complex **1** + H_2O_2, neither by complex **1** nor H_2O_2. The decrease of both the UV/VIS and EPR signals of $ABTS^{+\bullet}$ after certain time implies that $ABTS^{+\bullet}$ is also the substrate of the peroxidase activity of complex **1**. It has been suggested the formation of Ru(V)=O or Ru(IV)-OH species during the oxidation of hydroxyurea with H_2O_2 by an Ru(III) complex.[28] If the active intermediate of the peroxidase reactivity of complex **1** were Ru(V)=O, it would be detected by EPR. But our EPR experiments have not observed any new signal. And the characteristic absorption of a Ru(V)=O species at λ = 390 nm,[28] which is often indicative of the formation of a Ru(V)=O species, were not observed. This tends to suggest that a Ru(IV)-OH species is the active intermediate for the oxidation of ABTS and $ABTS^{+\bullet}$. However, Ru(V)=O cannot be completely ruled out because of the possibility that Ru(V)=O is a short-lived species and not accumulated enough to be detected by EPR and UV/VIS. The in-depth studies on the reaction are necessary for the suggestion. Currently, vibrational and mass spectroscopic investigations are underway to understand the catalytic mechanism.

Conclusions

A new anticancer octahedral Ru(III) complex, [Ru(III)-

(tpea)Cl_2](ClO_4) (**1**), with a tripodal tetraamine ligand, tpea = tris[2-(1-pyrazoyl)ethyl]amine, has been synthesized. X-ray crystallographic study revealed that complex **1** has a near octahedral geometry with the tetradentate ligand and two chloride ions. CV of complex **1** found two redox couples: one irreversible Ru(III)/Ru(II) process and one reversible Ru(IV)/Ru(III) process. Peroxidase activity was examined by observing the oxidation of 2,2'-azinobis(3-ethylbenzothiazoline)-6-sulfonic acid (ABTS) with hydrogen peroxide in the presence of complex **1**. Amount of $ABTS^{+\bullet}$ present during the reaction was monitored by UV/VIS and EPR spectroscopies. After the initiation of the peroxidase reaction, $ABTS^{+\bullet}$ concentration increases and then decreases after certain time, indicating that both ABTS and $ABTS^{+\bullet}$ are the substrates of the peroxidase activity of the Ru(III) complex. It is suggestive that Ru(IV)-OH species is the active intermediate for the oxidation of both ABTS and $ABTS^{+\bullet}$ though Ru(V)=O cannot be completely ruled out.

Acknowledgments. This research was supported by National Research Foundation of Korea Grant funded by the Korean Government (2009-0087304).

Supporting Information. Supplememtary material containing a table summarizing the crystal data is available at http://journal.kcsnet.or.kr.

References

1. Clarke, M. J. *Coord. Chem. Rev.* **2003**, *236*, 209-233.
2. Sakai, K.; Yamada, Y.; Tsubomura, T. *Inorg. Chem.* **1996**, *35*, 3163-3172.
3. Chatterjee, D. *Coord. Chem. Rev.* **2008**, *252*, 176-198.
4. Ward, M. D. *Coord. Chem. Rev.* **2006**, *250*, 3128-3141.
5. Concepcion, J. J.; Jurss, J. W.; Templeton, J. L.; Meyer, T. J. *J. Am. Chem. Soc.* **2008**, *130*, 16462-16463.
6. Dyson, P. J.; Sava, G. *J. Chem. Soc., Dalton Trans.* **2006**, 1929-1933.
7. Hartinger, C. G.; Zorbas-Seifried, S.; Jakupec, M. A.; Kynast, B.; Zorbas, H.; Keppler, B. K. *J. Inorg. Biochem.* **2006**, *100*, 891-904.
8. Lentz, F.; Drescher, A.; Lindauer, A.; Henke, M.; Hilger, R. A.; Hartinger, C. G.; Scheulen, M. E.; Dittrich, C.; Keppler, B. K.; Jaehde, U. *Anti-Cancer Drugs.* **2009**, *20*, 97-103.
9. Bratsos, L.; Jedner, S.; Gianferrara, T.; Alessio, E. *Chim. Intern. J. Chem.* **2007**, *61*, 692-697.
10. Alessio, E.; Mestroni, G.; Bergamo, A.; Sava, G. *Curr. Topics in Med. Chem.* **2004**, *4*, 1525-1535.
11. Blackman, A. G. *Polyhedron.* **2005**, *24*, 1-39.
12. Sorrell, T. N.; Jameson, D. L. *Inorg. Chem.* **1982**, *21*, 1014-1019.
13. Sheldrick, G. M. *SHELXTL-PLUS*; Crystal Structure Analysis Package, Bruker Analytical X-Ray, Madison, WI, USA, 1997.
14. Maneiro, M.; Bermejo, M. R.; Sousa, A.; Fondo, M.; Gonzalez, A. M.; Sousa-Pedrares, A.; McAuliffe, C. A. *Polyhedron* **2000**, *19*, 47-54.
15. Zipplies, M. F.; Lee, W. A.; Bruice, T. C. *J. Am. Chem. Soc.* **1986**, *108*, 4433-4445.
16. Scarpellini, M.; Toledo, C. T., Jr.; Neves, A.; Ellena, J.; Castellano, E. E.; Franco, D. W. *Inorg. Chim. Acta* **2004**, *357*, 707-715.
17. Murali, M.; Mayilmurugan, R.; Palaniandavar, M. *Eur. J. Inorg. Chem.* **2009**, 3238-3249.
18. Che, C.-M.; Yam, V. W.-W.; Mak, T. C. W. *J. Am. Chem. Soc.* **1990**, *112*, 2284-2291.
19. Kojima, T.; Amano, T.; Ishii, Y.; Ohba, M.; Okaue, Y.; Matsuda, Y. *Inorg. Chem.* **1998**, *37*, 4076-4085.
20. Sugimoto, H.; Matsunami, C.; Koshi, C.; Yamasaki, M.; Umakoshi, K.; Sasaki, Y. *Bull. Chem. Soc. Japan* **2001**, *74*, 2091-2099.
21. Hartshorn, R. M.; House, D. A. *J. Chem. Soc., Dalton Trans.* **1998**, 2577-2588.
22. Corey, E. J.; Bailar, J. C., Jr., *J. Am. Chem. Soc.* **1959**, *81*, 2620-2629.
23. Bermejo, M. R.; Fernandez, M. I.; Gonzalez-Noya, A. M.; Maneiro, M.; Pedrido, R.; Rodriguez, A. J.; Garcia-Monteagudo, J. C.; Donnadieu, B. *J. Inorg. Biochem.* **2006**, *100*, 1470-1478.
24. Maneiro, M.; Bermejo, M. R.; Fernández, M. I.; Gómez-Fórneas, E.; González-Noya, A. M.; Tyryshkin, A. M. *New J. Chem.* **2003**, *27*, 727-733.
25. Bermejo, M. R.; Fernández, M. I.; Gómez-Fórneas, E.; González-Noya, A.; Maneiro, M.; Rosa, P.; Rodríguez, M. J. *Eur. J. Inorg. Chem.* **2007**, 3789-3797.
26. Solis-Oba, M.; Ugalde-Saldivar, V. M.; Gonzalez, I.; Viniegra-Gonzalez, G. *J. Electroanal. Chem.* **2005**, *579*, 59-66.
27. McGarvey, B. R. *Coord. Chem. Rev.* **1998**, *170*, 75-92.
28. Chatterjee, D.; Nayak, K. A.; Ember. E.; van Eldik, R. *J. Chem. Soc., Dalton Trans.* **2010**, *39*, 1695-1698.